

# **CHAPTER 6**

## **GROUNDWATER SALINITY DISTRIBUTION AND IMPACT TO AGRICULTURE ACTIVITIES**

### **6.1 Introduction**

This chapter assesses the impact of groundwater salinity distribution and oil palm tree tolerance towards groundwater salinity in Carey Island by using empirical relationships of subsurface resistivity and TDS that were derived in Chapter 5. The assessment of seawater intrusion in this study area was conducted using 3-D subsurface resistivity and conductivity slices, which are transformed from sequential 2-D resistivity and conductivity images. The two types of land cover areas of concern in this assessment are the still-intact mangrove forest reserve and the severe coastal erosion area. This study also assesses the impact of future seawater level rise on the groundwater aquifer system and oil palm tolerance towards groundwater salinity in Carey Island. A flow chart for this chapter is shown in Figure 6.1.

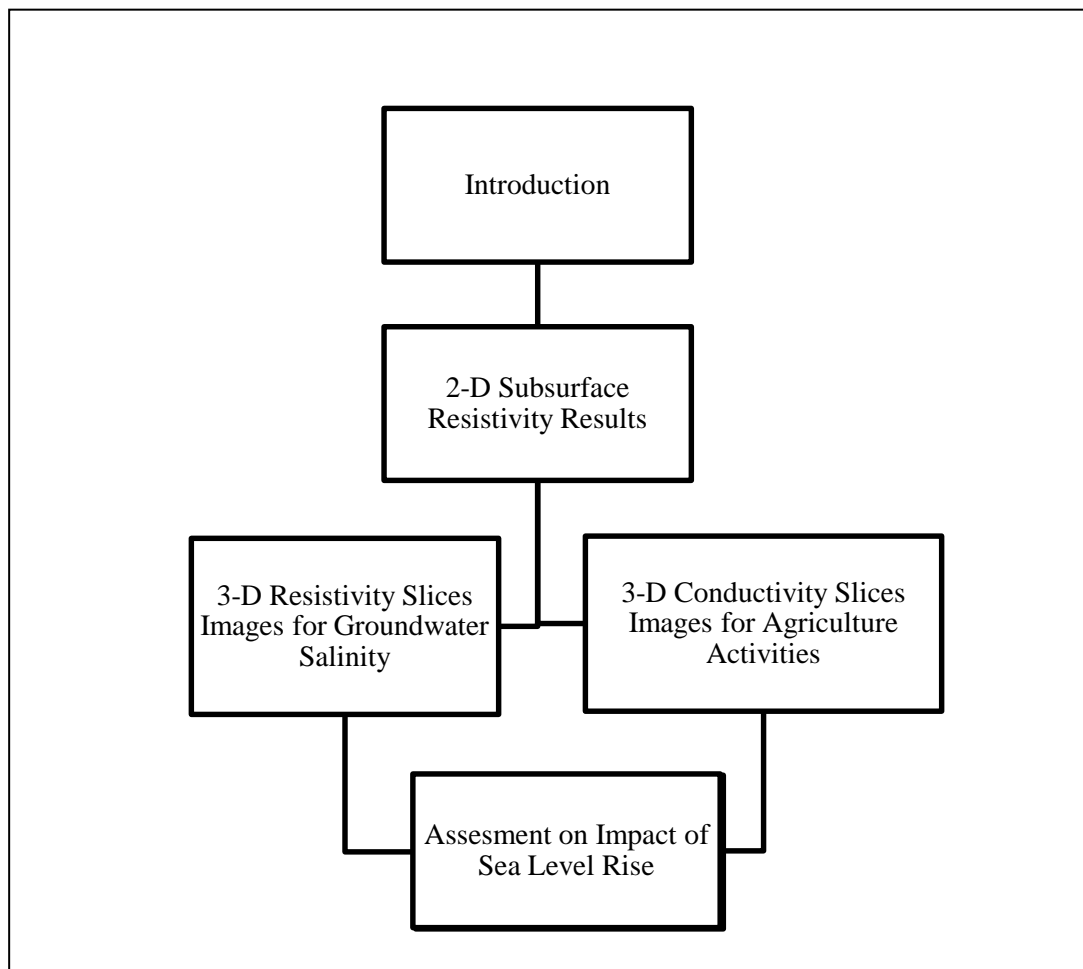


Figure 6.1: Flow chart for the assessment of groundwater salinity and agriculture activities

## 6.2 2-D subsurface resistivity results (second phase)

In the second phase subsurface resistivity measurements, a number of seventeen resistivity lines, L1-L1' up to L17-L17', were set up, and the lines crossing the wells areas indicated in the first phase and those not crossing other wells are as shown in Figure 6.2. Subsurface resistivity apparent data are inverted to resistivity images model by using Res2Dinv software. Seventeen resistivity images model results are shown in Figures 6.3 until 6.19. Resistivity images for all profiles started at a depth of 1.25 m from the ground surface and ended at a depth of 60.0 m. The entire resistivity images depth profile obtained can be considered as fully saturated with groundwater.

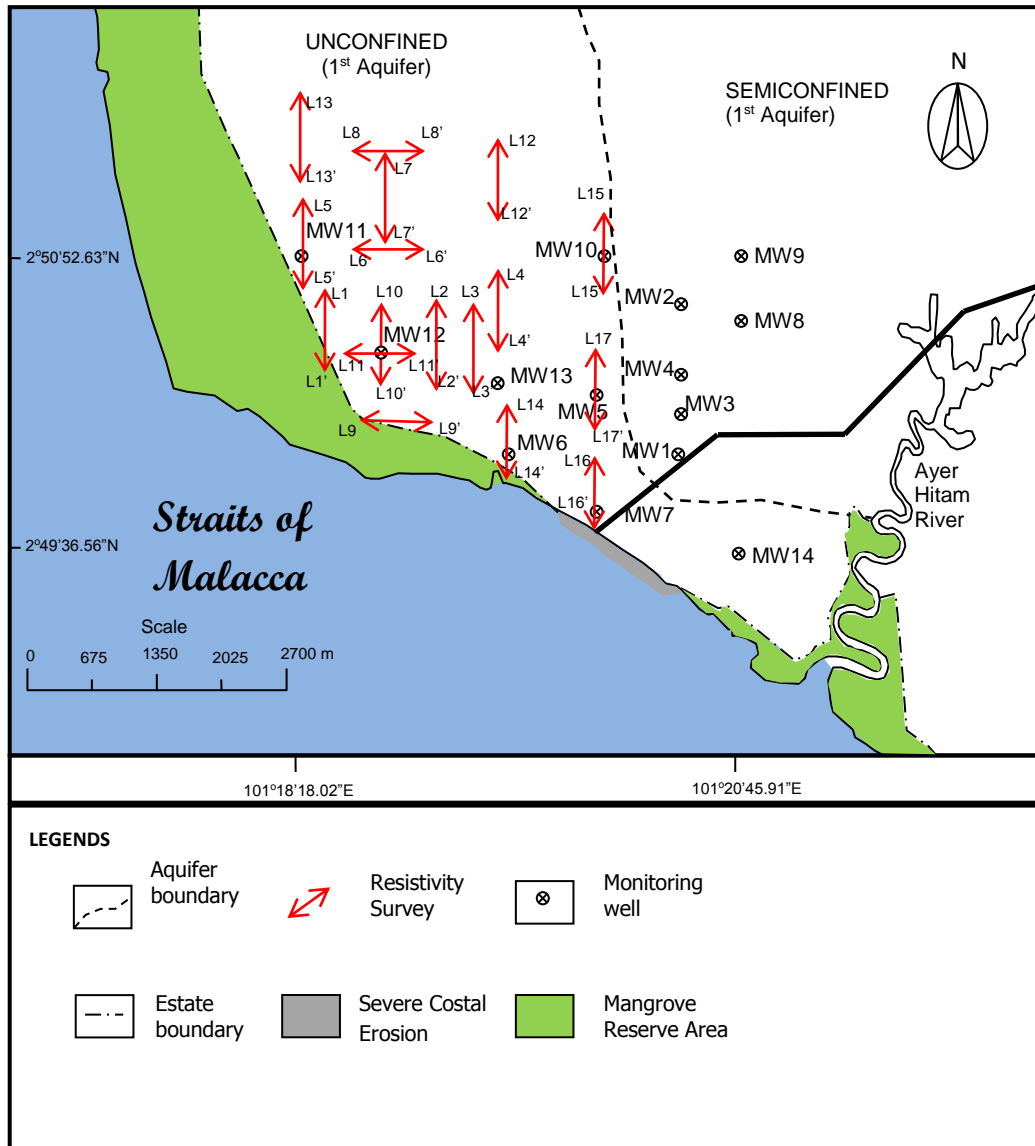


Figure 6.2: Locations of resistivity survey and monitoring wells in study area. Some of resistivity survey in second phase crossed over the monitoring wells as well as in first phase

Three schematic gradient contour colours were used to classify the groundwater salinity degree as derived in Equation (5.2) in the subsurface resistivity images. Blue denoted a subsurface resistivity  $>10 \Omega.m$  and representing freshwater. Green denoted 3 to  $10 \Omega.m$  and representing brackish water. Red denoted  $<3.0 \Omega.m$  and representing saline water. The subsurface resistivity profiles were selected in five different locations, outlined below. They were chosen in order to represent variations in the two distinctively different land cover settings overlying the unconfined aquifer.

- a) Profiles L6-L6', L7-L7', and L8-L8' were located in the middle aquifer with mangrove cover in the west and south.
- b) Profiles L1-L1' and L5-L5' were located in the west of the aquifer surrounded by mangrove.
- c) Profile L14-L14' was located close to the estuary where the agricultural hydraulic structures (tidal gate, bund, and main canal) were found.
- d) Profiles L15-L15' and L17-L17' were located in the middle east of the aquifer with mangrove uncovered in the east and south.
- e) Profile L16-L16' was located close to a heavily eroded coastal belt in the south.

### **6.2.1 Resistivity profiles L6-L6', L7-L7' and L8-L8'**

These profiles were located in the middle of the unconfined system in the island about 1.6 to 2.5 km from the south and west coasts (Figure 6.2). Freshwater thickness (blue coded) varied in depth from 28 m (minimum) (Figure 6.10) to 40 m (maximum) (Figures 6.8 and 6.9) with the overall resistivity within the freshwater lens ranging from 10 to  $55 \Omega.m$ . Underneath the freshwater, brackish water (green coded) was found overlying saline water (red coded) separated by an undulating saline-brackish water interface.

### **6.2.2 Resistivity profiles L1-L1' and L5-L5'**

These profiles were located close to mangrove areas in the west (Figure 6.2). Resistivity profiles L1-L1' showed dominance of brackish water to a depth of 20 m. The brackish water can be found below the saline water. Freshwater lenses were scattered about throughout the resistivity profile L5-L5' in approximately 10 m thickness with resistivity between 10.0 and 24  $\Omega$ .m. Saline water (red coded) was dominantly found in the 19 m depth (with resistivity below 3  $\Omega$ .m) overlain by brackish water (green coded). This groundwater salinity exhibited almost horizontal interfaces between each other (Figure 6.7).

### **6.2.3 Resistivity profile L14-L14'**

This profile (Figure 6.16), about 98 m away from the coast, crossed over MW6 (Figure 6.2). Close to it were found some of the estuarine hydraulic structures such as open canals and tidal gates. In the shallow subsurface was saline water at 2.5 to 10 m deep with resistivity value between 0.5 and 3.0  $\Omega$ .m. Brackish water was predominant below the saline water in the 400 m distance of the traverse line with resistivity between 3 and 10  $\Omega$ .m.

### **6.2.4 Resistivity profile L15-L15'**

This profile (Figure 6.17) crossed over MW10 (Figure 6.2). The nearest coastal area to the study area was about 2.2 km away in the south beneath the open mangrove with severely eroded land cover. Brackish water (green) was thin, overlying the saline water (red coded) which was predominantly found with low resistivity ( $< 3 \Omega$ .m) below the 10 m depth. The freshwater lens appeared only 5 m thick.

### 6.2.5 Resistivity profile L16-L16'

This profile (Figure 6.18) was located 15 m away from the coast crossed over MW7 (Figure 6.2). In the distance about 3.2 km along coastal area was found heavily deforested and eroded of coastal mangrove. Freshwater was < 10 m thick with resistivity exceeding 10  $\Omega$ .m. The saline water was, however, more prominent in the subsurface with low resistivity (< 3 $\Omega$ .m).

In relative profile comparison, it was noted that all profiles have freshwater in varying thickness except for L13-L13'. Profiles L5-L5'; L14-L14'; L15-L15' and L4-L4' appeared to have thinner freshwater compared with L6-L6'; L7-L7' and L8-L8'. Both L15-L15' and L16-L16', as noted, were located in the eroded side (west) of the study area. Profile L6-L6'; L7-L7' and L8-L8' have practical implications to the freshwater production wells that could be constructed in the vicinity of the traverse line at depths exceeding 20 m.

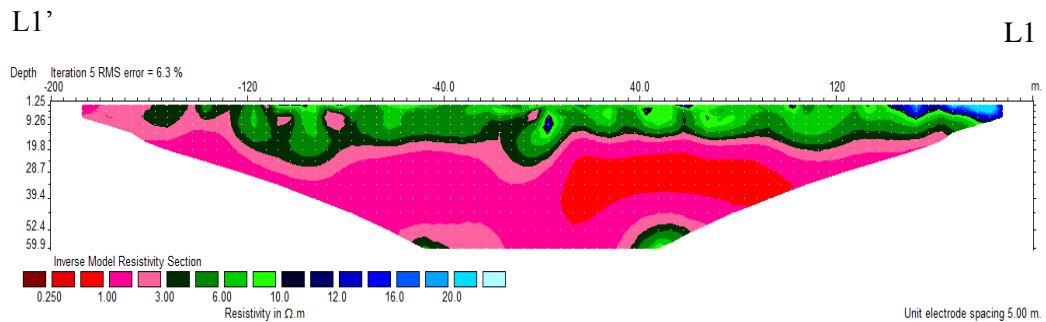


Figure 6.3: Electrical resistivity image for profile L1-L1'

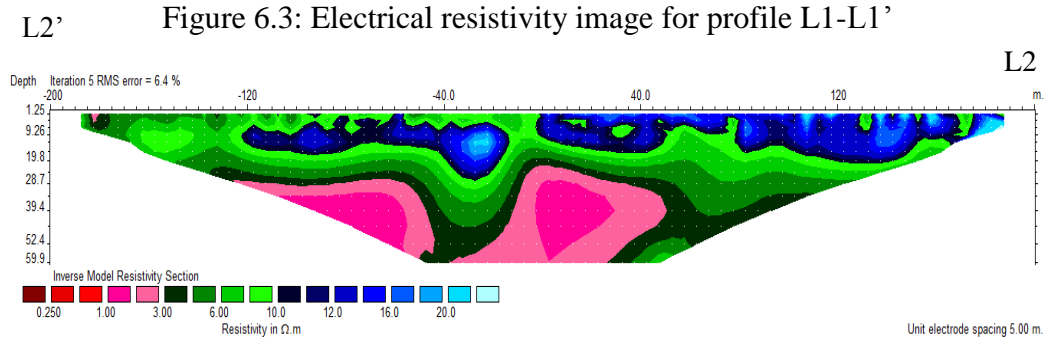


Figure 6.4: Electrical resistivity image for profile L2-L2'

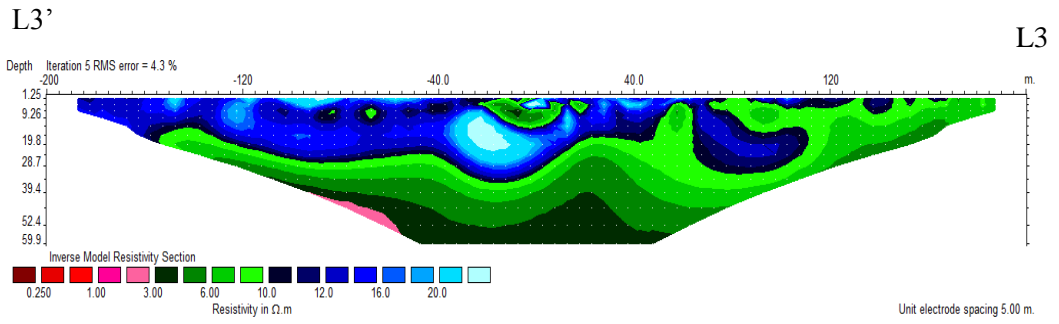


Figure 6.5: Electrical resistivity image for profile L3-L3'

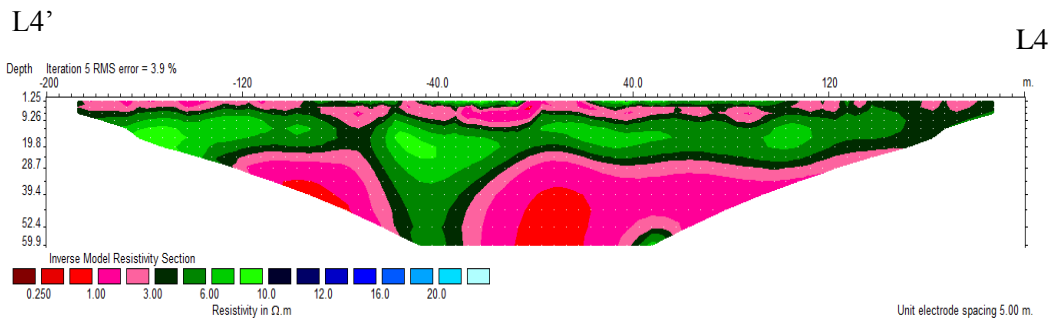


Figure 6.6: Electrical resistivity image for profile L4-L4'

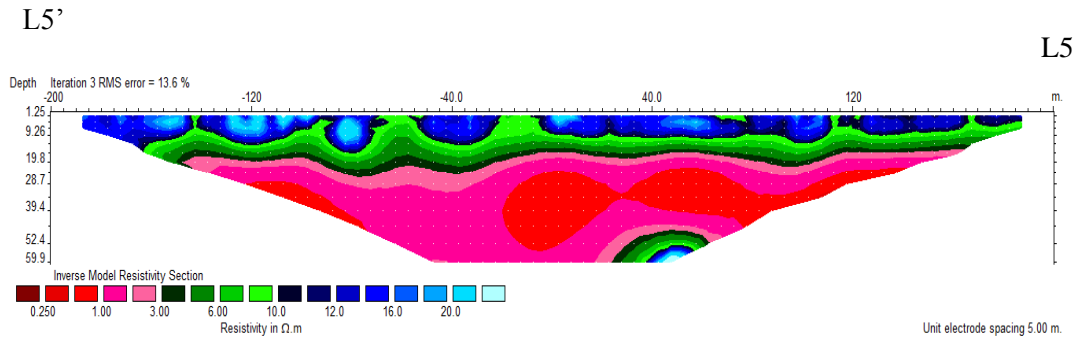


Figure 6.7: Electrical resistivity image for profile L5-L5'

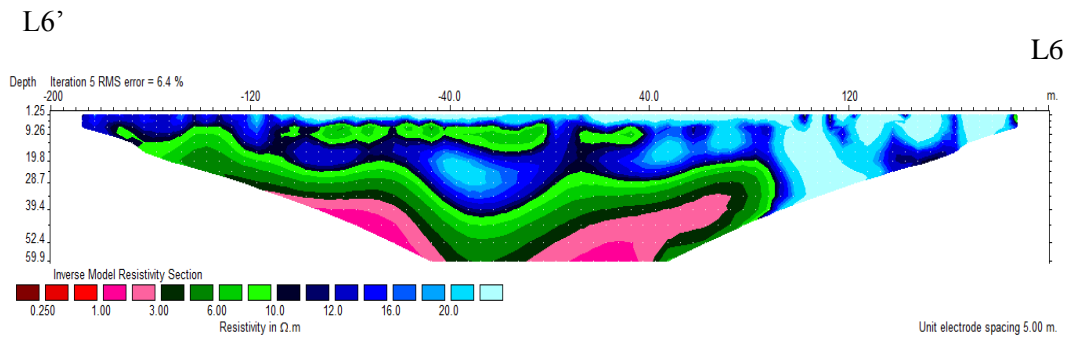


Figure 6.8: Electrical resistivity image for profile L6-L6'

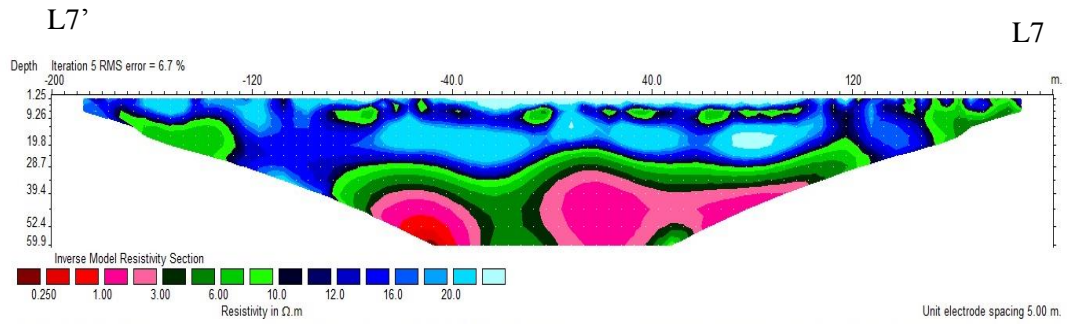


Figure 6.9: Electrical resistivity image for profile L7-L7'

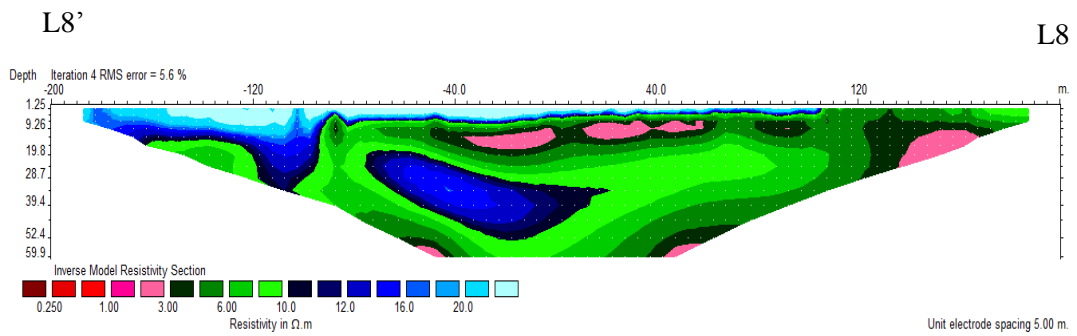


Figure 6.10: Electrical resistivity image for profile L8-L8'

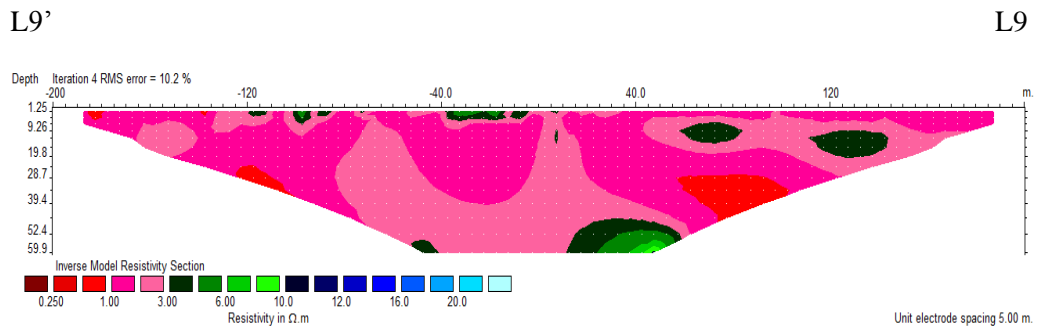


Figure 6.11: Electrical resistivity image for profile L9-L9'

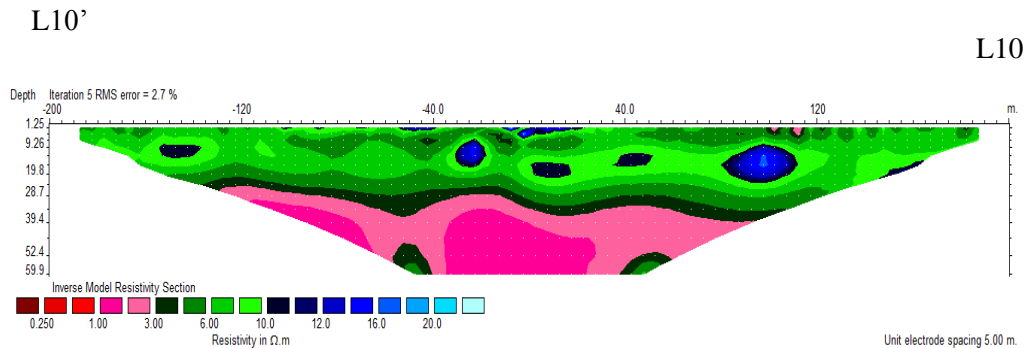


Figure 6.12: Electrical resistivity image for profile L10-L10'

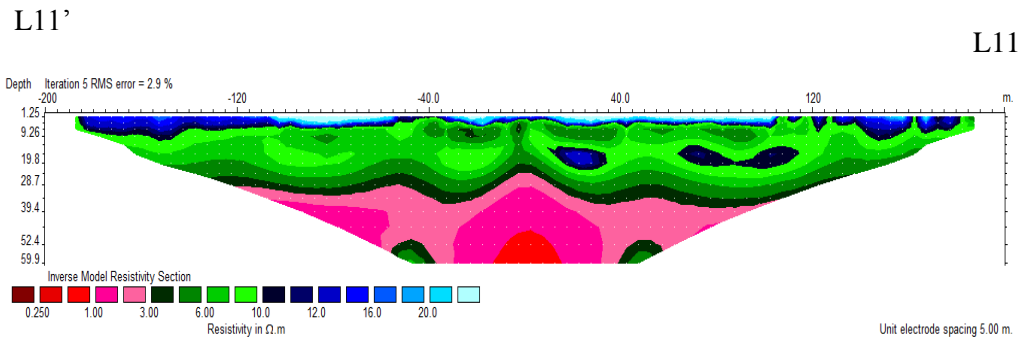


Figure 6.13: Electrical resistivity image for profile L11-L11'

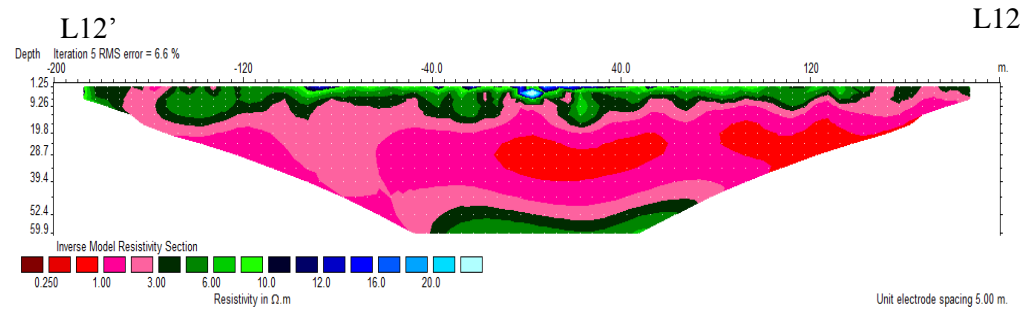


Figure 6.14: Electrical resistivity image for profile L12-L12'

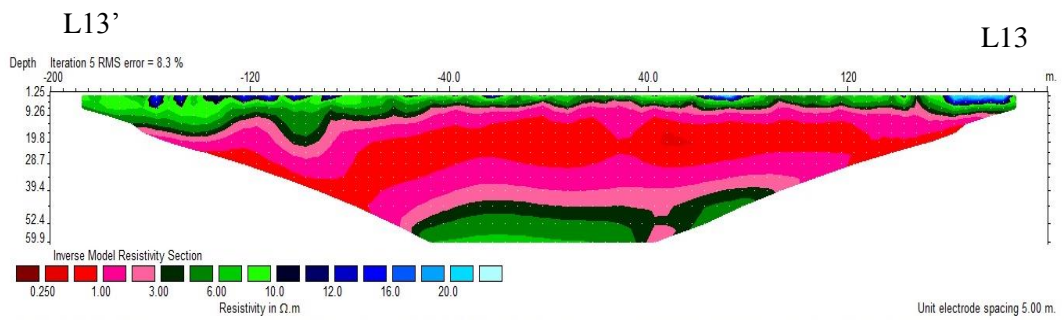


Figure 6.15: Electrical resistivity image for profile L13-L13'

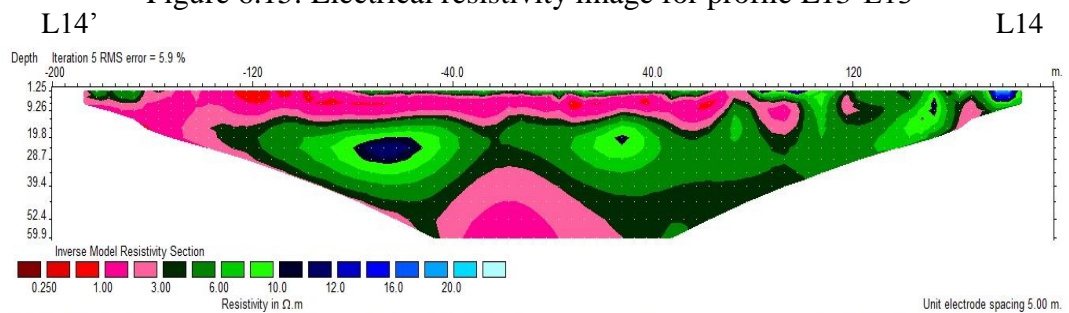


Figure 6.16: Electrical resistivity image for profile L14-L14'

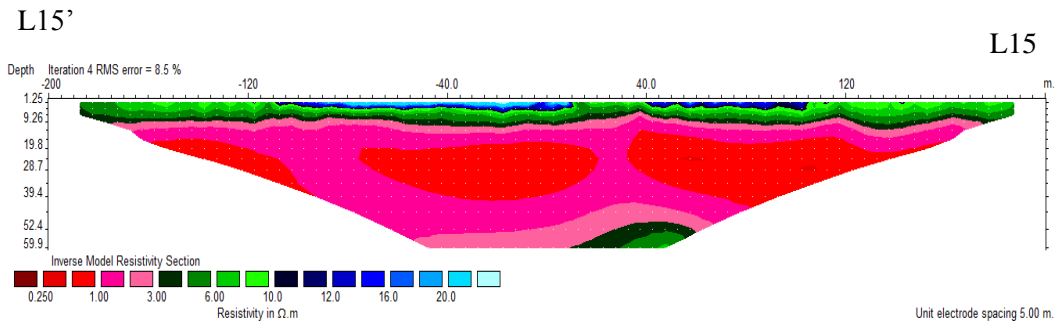


Figure 6.17: Electrical resistivity image for profile L15-L15'

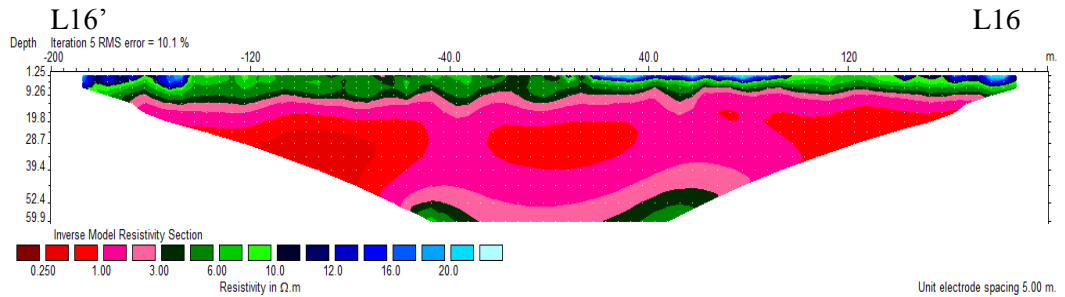


Figure 6.18: Electrical resistivity image for profile L16-L16'

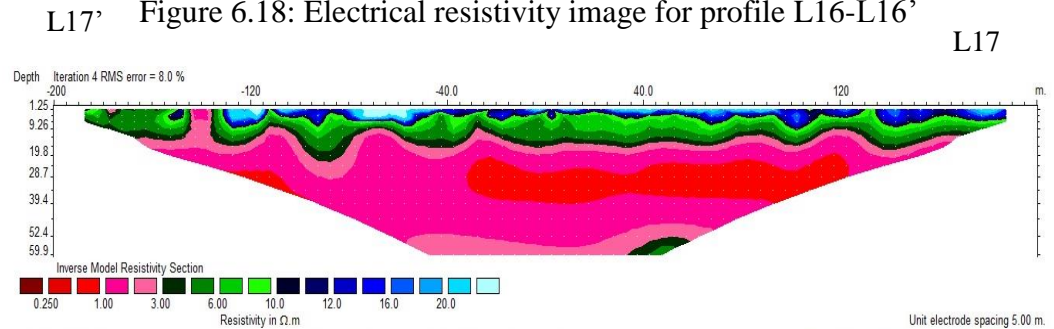


Figure 6.19: Electrical resistivity image for profile L17-L17'

### 6.3 3-D resistivity mapping for groundwater salinity distribution

In order to obtain a better shape and distribution of the groundwater salinity degree, a simplified 3-D resistivity model had been developed. The sequence of 2-D resistivity images (Figures 6.3 to 6.19) were transformed into 3-D resistivity slice images by using the Kriging interpolating technique available in Surfer version 8 software.

Two and three dimensional analysis of hydraulic head of the groundwater using the observed groundwater level is shown in Figure 6.20 and 6.21 respectively. 3-D resistivity slice images showing the resistivity distribution of groundwater salinity for depths between 1.25 to 42.34 m are shown in Figures 6.22, 6.23 and 6.24. Resistivity distribution for groundwater salinity is represented by using different colour codes. The

colour codes used are blue for freshwater ( $> 10 \Omega.m$ ), green for brackish water (3 to 10  $\Omega.m$ ), and red for saline water ( $< 3 \Omega.m$ ).

Resistivity slice images for the 1.25 and 5.0 m depths are shown in Figures 6.22 and 6.23(a), respectively. In this water zone, freshwater (horizontal) coverage was about 3.0  $km^2$ , one third of the coverage for brackish–saline water (about 11.0  $km^2$  see Table 6.1). The dominance of water brackishness and salinity was due to seepage from the agriculture drainage [profile L14–L14' (near MW6), profile L7–L7' and profile L8–L8' shown in Figure 6.2]. The freshwater contamination in the shallow aquifer was caused by seawater infiltration from the agriculture drainage. In the same depths (1.25 to 5.0 m) the saline water occurred mostly in the southwest (in the reserved mangrove) due to tides moving from the mangrove to the bunds separating it from the oil palm cultivation. In the past, the bunds in the mangrove had been frequently damaged, causing the surface saline water to overflow into the oil palm plantation, thus contributing to the groundwater salinity in the southwest area. An important finding in the study is the indication of freshwater availability in the mid-study area as deep as 30 m into the groundwater aquifer (Figure 6.24). For depths exceeding 10 m the saline water occurrence is mainly due to seawater intrusion (Table 6.1). The results of the groundwater salinity degree (3-D) and area coverage are summarized in Table 6.1 with reference to water depths.

3-D resistivity model in this study showed that the freshwater lens distribution did not conform to the freshwater-seawater hydraulic gradient as usually described by other studies. Praveena and Aris (2010) as well as White and Falkland (2010) reported that normally, freshwater lenses thickly occurred in the middle of the island and radials flowed towards the edge of the coastal island. In the present case study, the contrary was found. Saline water was dominant in some aquifers from the coast (Figure 6.23). In other areas, 30 m thick freshwater was found [Figure 6.24 (g)]. The 3-D resistivity slice

images for depths below 5 m [Figure 6.23 (a)] on the east side of the unconfined aquifer system showed the dominance of brackish and saline waters over the groundwater aquifer. The land transformation in this area, which showed severe coastal erosion especially in the east-south area, decreased the original level of the coastal surface. This transformation was believed to have changed the hydrogeology of the island, which receives seawater pressure all the time.

In contrast, in the west-south areas, which were still preserved with large-scale reserved mangrove areas, the geomorphology of the coastal area was sustained. Seawater intrusion inland was also prevented. Bann (1998) highlighted the natural-barrier action of mangroves against shoreline erosion. Mangroves stabilize fine sediments by plant root binding as well as stabilizing deposited soil and vegetative matter. Mangroves also dissipate erosion forces (e.g., wave and wind) and trap sediments. Large-scale deforestations of mangroves result in coastal flooding and erosion. As from hydrogeological aspects, groundwater recharge refers to the movement (usually downward) of surface water into the groundwater flow system. Water moving from mangroves into aquifers can maintain part of the shallow groundwater system by two ways. First is by supplying water to surrounding areas and sustaining the water table. Second is by eventually moving into the deep groundwater system, which is a long-term water resource. Mangroves prevent saline water intrusion into shallow groundwater supply systems as well. According to Blasco et al., (2005), mangroves usually tolerate higher salinity than non-mangrove plants (Table 6.2). Mangrove plants that grow close to the sea are more tolerant towards salinity, for example *Avicennia marina* if compared with *Avicennia integrata*, which is less tolerant. Sarawasthy et al., (2009) conducted the study for determining diversity and estimate biomass of selected mangrove trees in nine study plots (50 m<sup>2</sup>) on Carey Island. The study found that *Avicennia alba* was the most dominant species followed by *Rhizophora mucronata* and *Rhizophora apiculata*.

Referring to Table 6.2, mangrove trees in Carey Island can be tolerant to intermediate saline concentration.

Table 6.1: Summary of groundwater salinity and area coverage/dominancy

| Vertical Depth of Water Zone (m) | Horizontal Area Coverage (Km <sup>2</sup> ) of Groundwater Salinity |  | Freshwater Area Dominancy | Remarks  |
|----------------------------------|---|--|---------------------------|--|
|                                  | Freshwater, >10 Ω.m (Bluecolor)                                     | Brackish-Saline Water, ~0-10 Ω.m (Green-Redcolors) |                           |  |
| 1.25                             | 3.50  | 10.82  | West to East              | Brackish-saline water caused by seepage from main canal and agriculture drainage (Figure 6.20)               |
| 5.0                              | 3.25  | 11.07  | West and Middle           | Brackish-saline water caused by seepage from main canal and agriculture drainage [Figure 6.21(a)]            |
| 10.80                            | 1.00  | 13.32  | Middle                    | Brackish-saline water caused by seawater intrusion mostly from severely eroded area [Figure 6.21 (b)]        |
| 14.10                            | 0.75  | 13.57  | Middle                    | Brackish-saline water caused by seawater intrusion mostly from severely eroded area (east) [Figure 6.21 (c)] |
| 21.80                            | 0.40  | 13.92  | Middle                    | Brackish-saline water caused by seawater intrusion [Figure 6.21 (d)]   |
| 31.10                            | 0.38  | 13.94  | Middle                    | Brackish-saline water caused by seawater intrusion [Figure 6.22 (f)]   |
| 36.45                            | 0.35  | 13.97  | Middle                    | Brackish-saline water caused by seawater intrusion [Figure 6.22 (g)]   |
| 42.34                            | -   | 14.32  | -                         | Brackish-saline water caused by seawater intrusion [Figure 6.22 (h)]   |

Table 6.2: Types of plants in different water qualities (Blasco et al., 2005)

| Environment          | Saltwater   | Intermediate   | Fresh water   |
|----------------------|---|--|---|
| Saline concentration | 30–45 ppt   | 20–30 ppt  | Lower than 20 ppt   |
| TDS                  | 28–43 g/L   | 19 – 28 g/L  | < 19 g/L  |
| Types of plants      | <i>Avicennia marina</i><br><i>Rhizophora mangle</i><br><i>Bruguiera gymnorrhiza</i><br><i>Lagunculari aracemosa</i><br><i>Sonneratia alba</i> | <i>Rhizophoraceae</i><br><i>Avicennia Alba</i><br><i>Avicennia officinalis</i><br><i>Excoecaria</i><br><i>Lumnitzera</i><br><i>Pelliciera</i><br><i>Xylocarpus</i> | <i>Avicennia integra</i><br><i>Heritierafomes</i><br><i>Sonneratia lonceolata</i> |

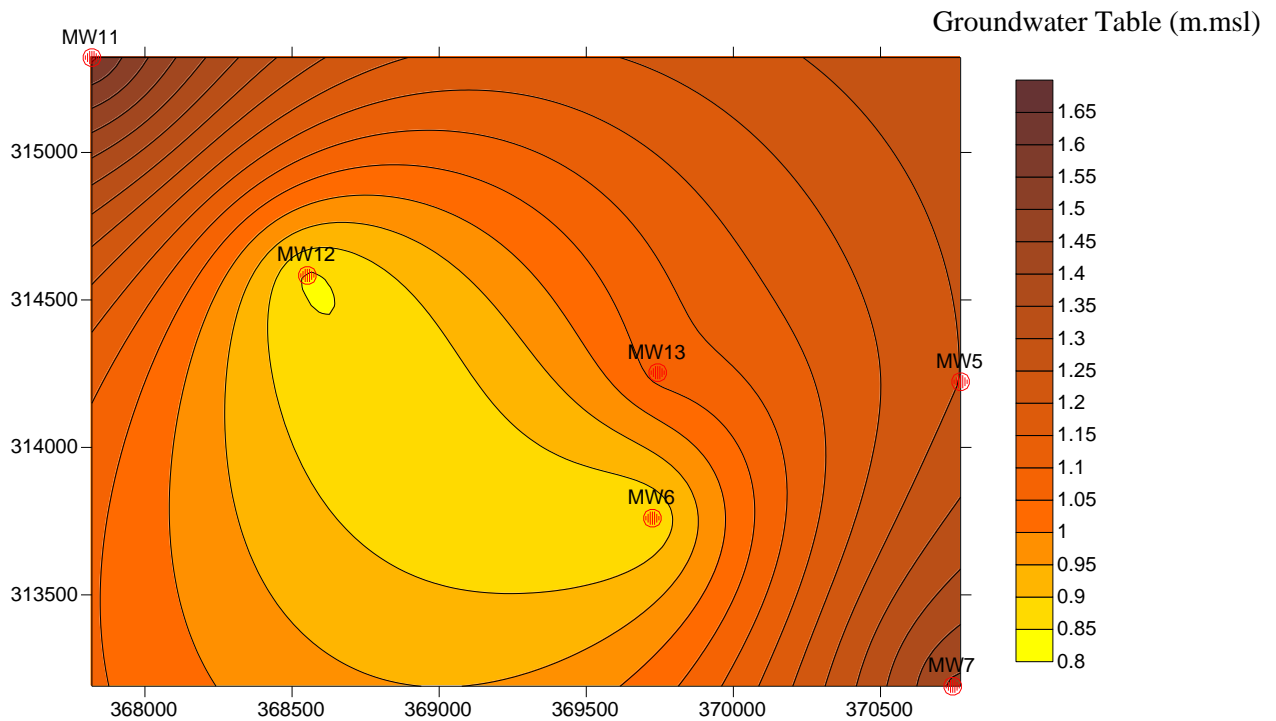


Figure 6.20: Two dimensional analysis of hydraulic head of the groundwater using the observed groundwater level

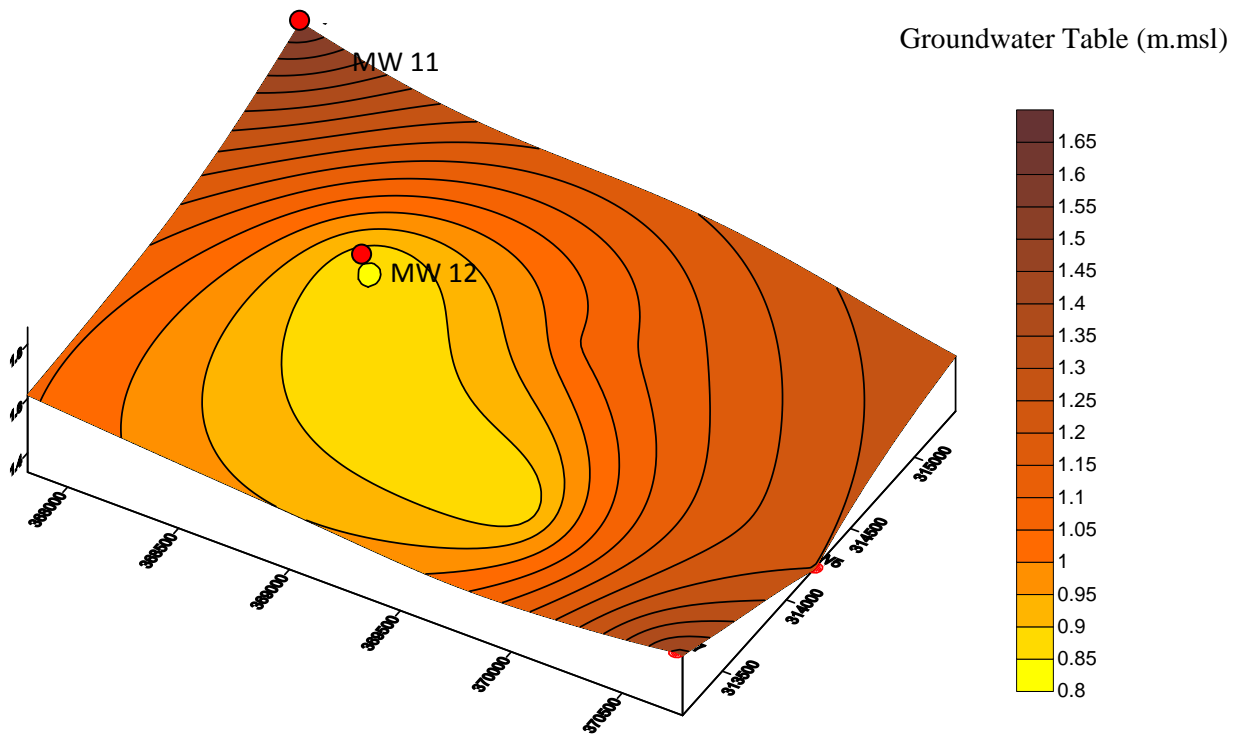


Figure 6.21: Three dimensional analysis of hydraulic head of the groundwater using the observed groundwater level

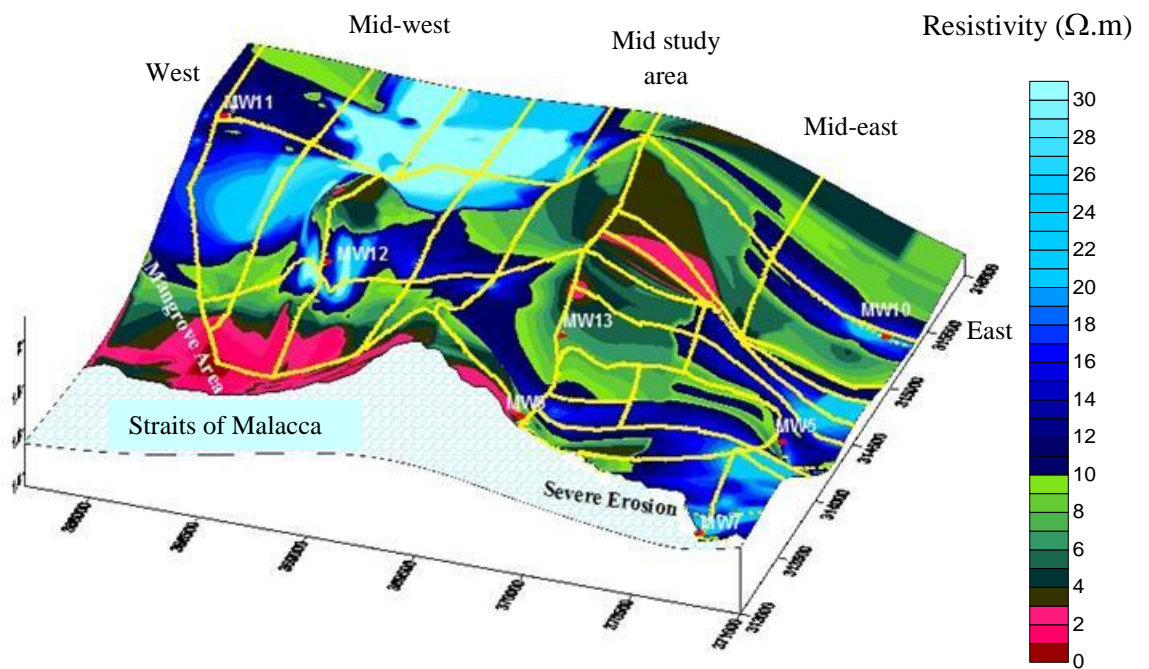


Figure 6.22: Resistivity distribution relative to elevation at 1.25 m depth and agriculture drainage system

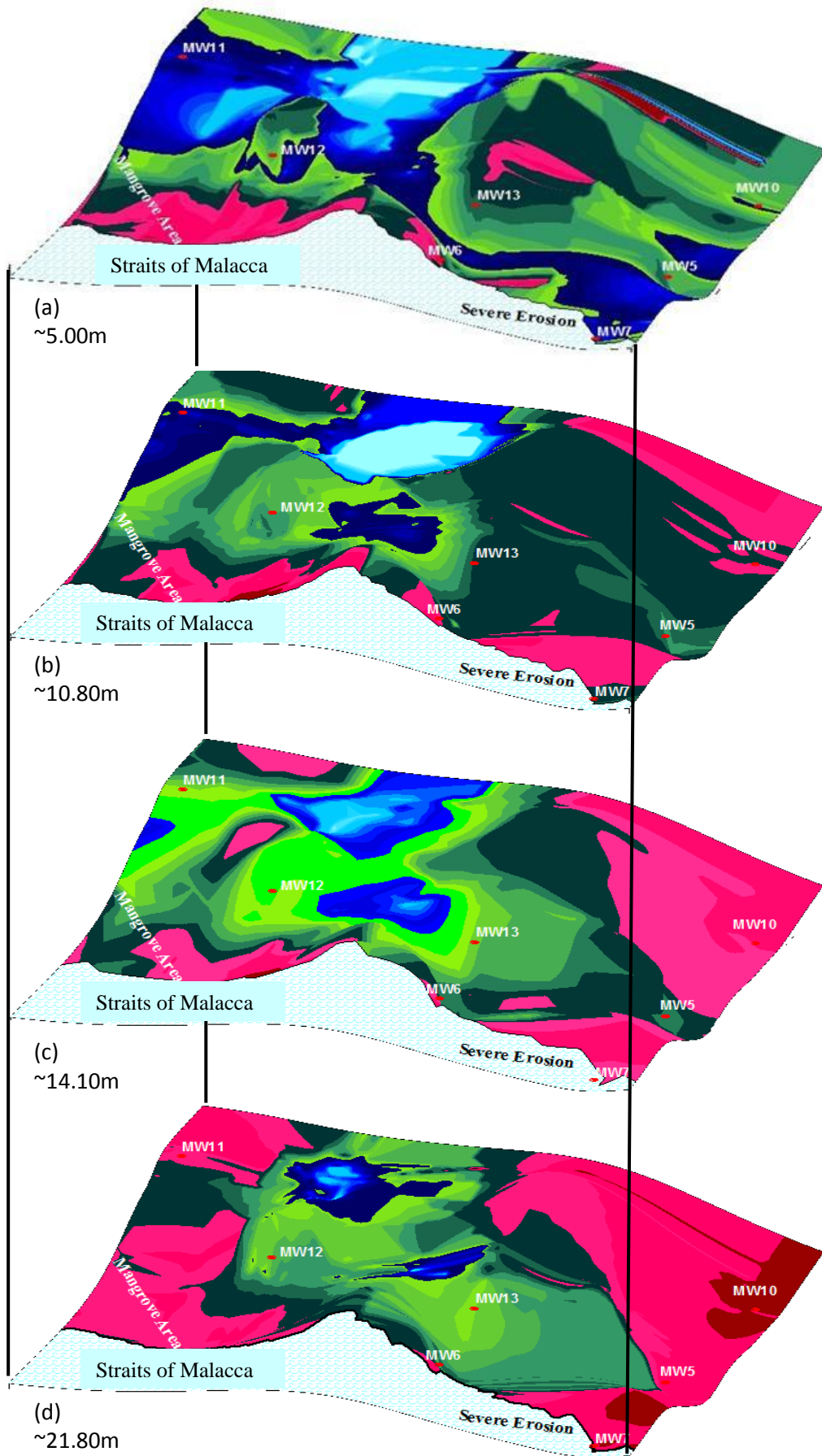


Figure 6.23: Resistivity distribution relative to elevation from 5.0 to 21.8 m depth

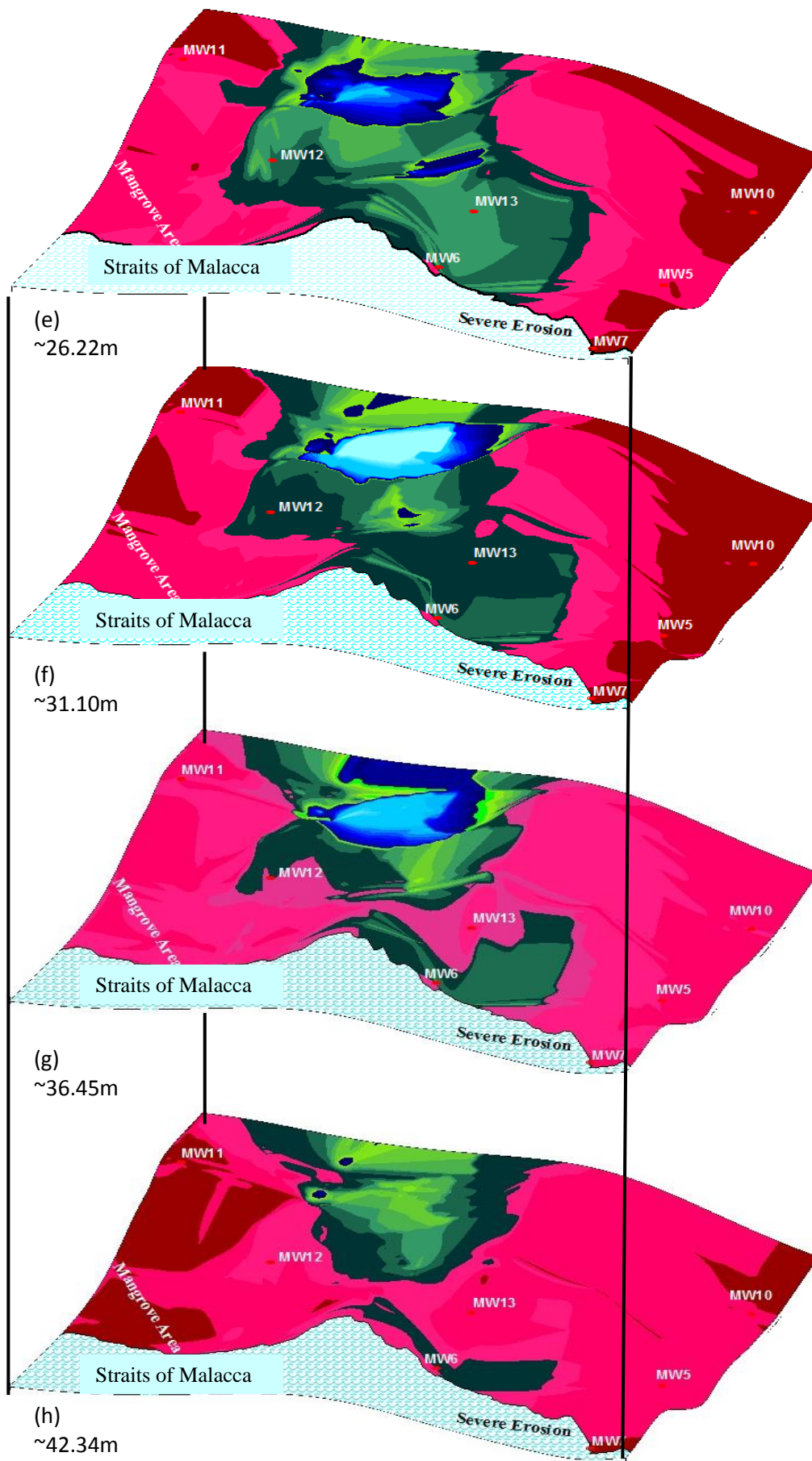


Figure 6.24: Resistivity distribution relative to elevation from 26.22 to 42.34 m depths

#### **6.4 3-D conductivity mapping for the suitability of oil palm cultivation towards salinity**

In this study, the 2-D conductivity inversion model is derived by taking the inverse of the subsurface resistivity data and calculates by using the Res2Dinv. The results of 2-D conductivity inversion model based on the following classification of the suitability of oil palm towards salinity proposed by Abdul Ghani et al., (2004) are shown in Figures 6.25 until 6.41. Conductivity distributions for the suitability of oil palm towards salinity were represented by using different colour codes. The colour codes used were blue for suitable ( $> 0.4$  S/m), green for moderately suitable ( $0.4$  S/m  $< C < 0.2$  S/m), and red for not suitable ( $< 0.2$  S/m).

In order to obtain a better shape and distribution of suitability of oil palm towards salinity, a simplified 3-D conductivity model has been developed. The sequence of 2-D conductivity images (Figures 6.26 to 6.39) were transformed into 3-D conductivity slice images (Figures 6.42, 6.43 and 6.44) by using the Kriging interpolating technique available in Surfer version 8 software.

The 3-D conductivity slice images at the depths of 1.25 and 5.0 m [Figures 6.42 and 6.43 (a)] showed that more than 80% (Table 6.3) of the area with conductivity values of 0.2 S/m is suitable for oil palm plantation. The image also showed that some areas are moderately suitable and not suitable for plantation, especially along the main agricultural canal drainages (mid-study area) and areas near the coast with un-bund mangroves (west area). On the east side area with severe coastal erosion, there are more drainage lines which has accumulated a lot of freshwater from precipitation compared to the west side. This is why the shallow depths near the severe coastal area still exhibits suitable condition for oil palm cultivation. In addition, the severe erosion in the area was mitigated by the construction of man-made bund and well-developed roads that prevented the penetration of saline water into the plantation ground surface.

Contradictions to the west coastal mangrove side, saline water intrusion occurs during high tide when seawater floods the area. Mangrove plants that grow close to this coastal area are more tolerant towards salinity due to saline water intrusion. Behind the mangrove reserved area, man-made bunds were constructed to prevent saline water intrusion into the plantation area.

As for the severely eroded area on the west side, the moderate conductivity condition (0.2–0.4 S/m) appeared at a depth of 7.75 m. On the west side, a similar depth was still suitable for oil palm cultivation [Figure 6.43 (b)]. The conductivity value for the severely eroded area which is not suitable for oil palm plantation was at 14.10 m depth [Figure 6.43 (d)]. In the west side, where mangrove forests still existed, the conductivity value suitable for plantation was at 31.10 m depth [Figure 6.44 (g)]. The results of the conductivity distributions for the suitability of oil palm towards salinity and area coverage are summarized in Table 6.3 with reference to water depths.

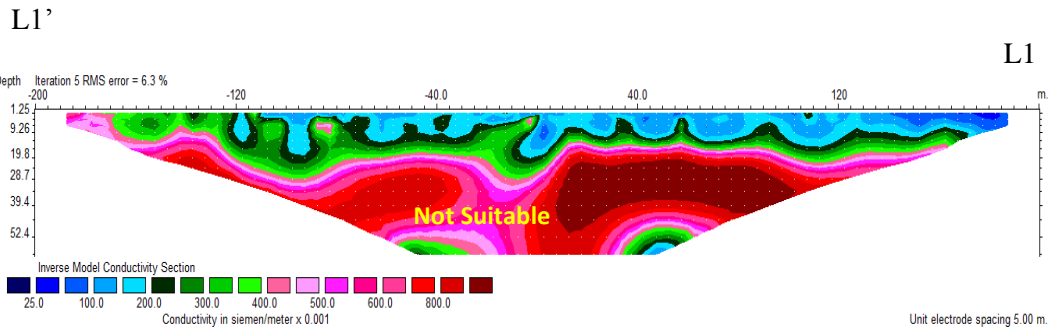


Figure 6.25: Conductivity image for profile L1-L1'

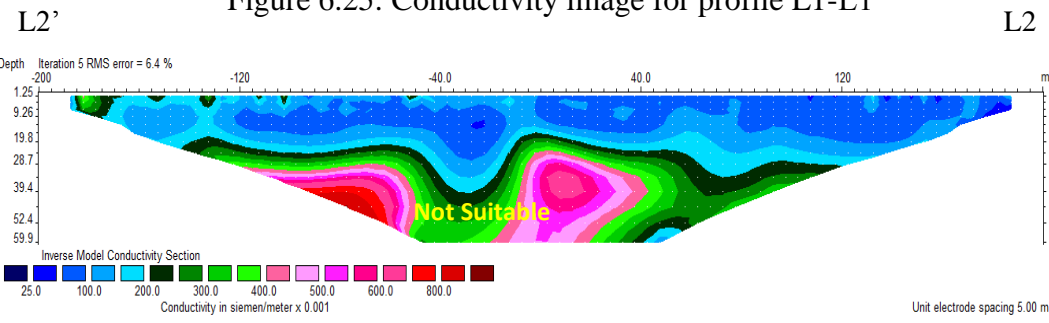


Figure 6.26: Conductivity image for profile L2-L2'

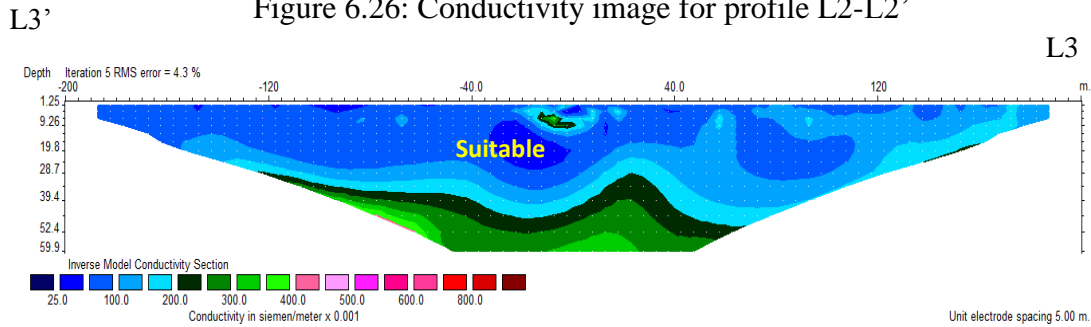


Figure 6.27: Conductivity image for profile L3-L3'

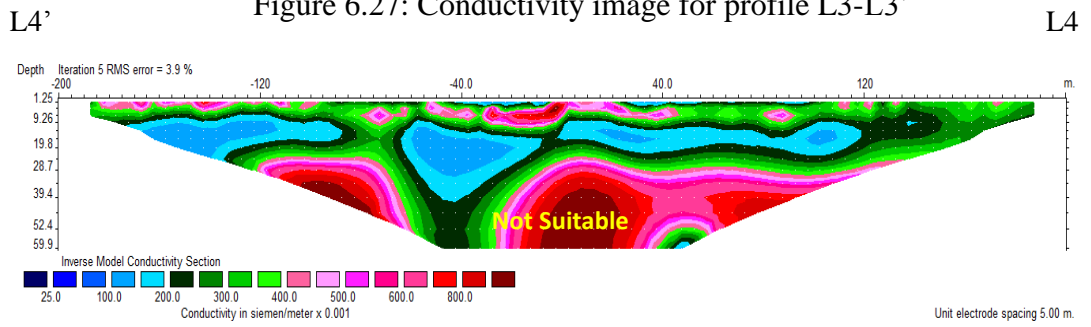


Figure 6.28: Conductivity image for profile L4-L4'

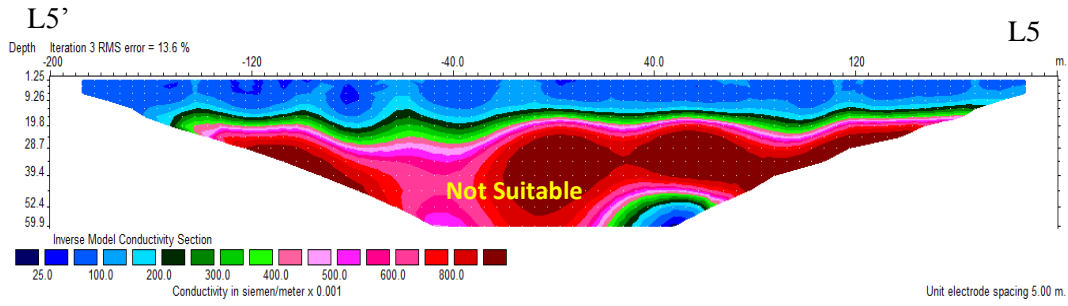


Figure 6.29: Conductivity image for profile L5-L5'

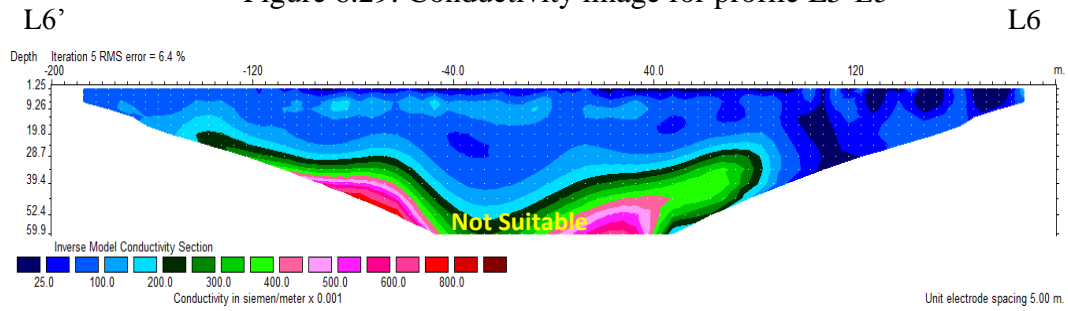


Figure 6.30: Conductivity image for profile L6-L6'

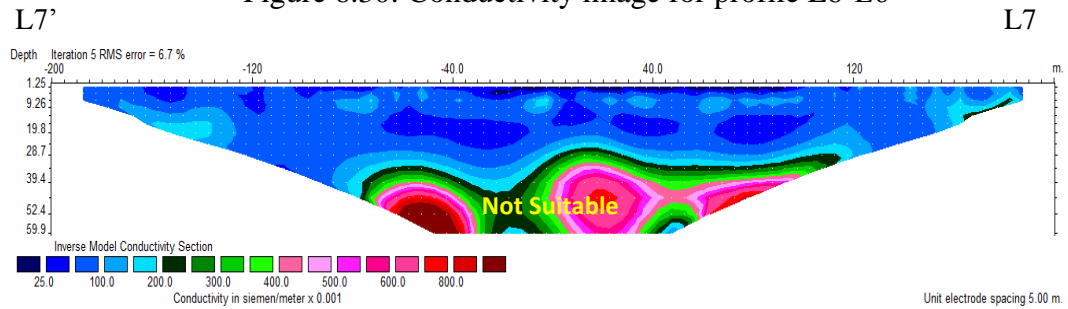


Figure 6.31: Conductivity image for profile L7-L7'

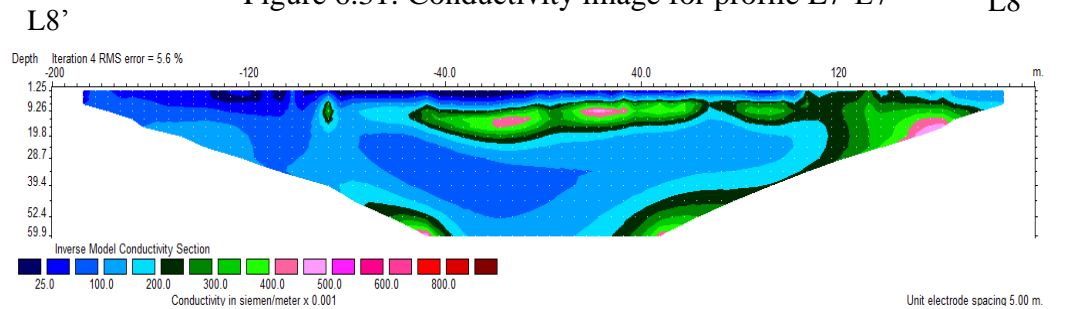


Figure 6.32: Conductivity image for profile L8-L8'

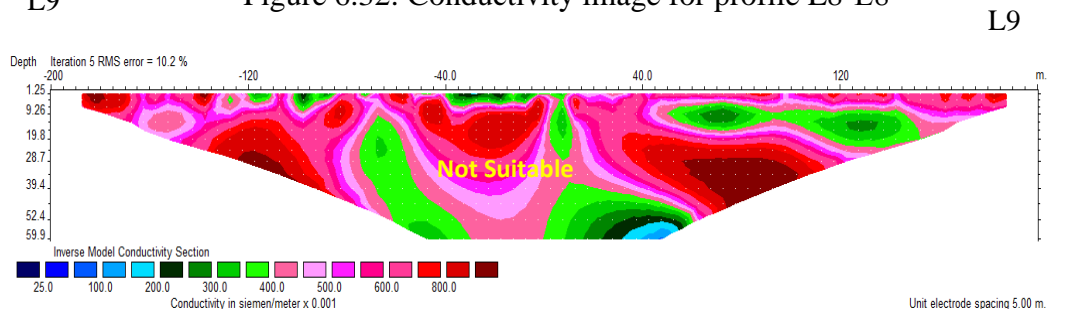


Figure 6.33: Conductivity image for profile L9-L9'

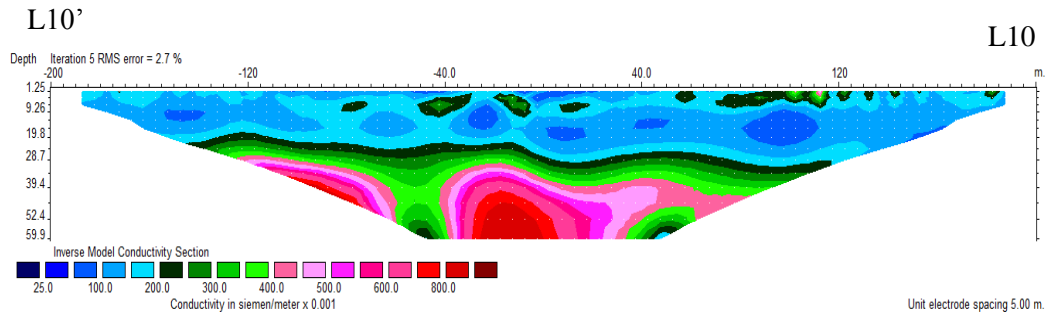


Figure 6.34: Conductivity image for profile L10-L10'

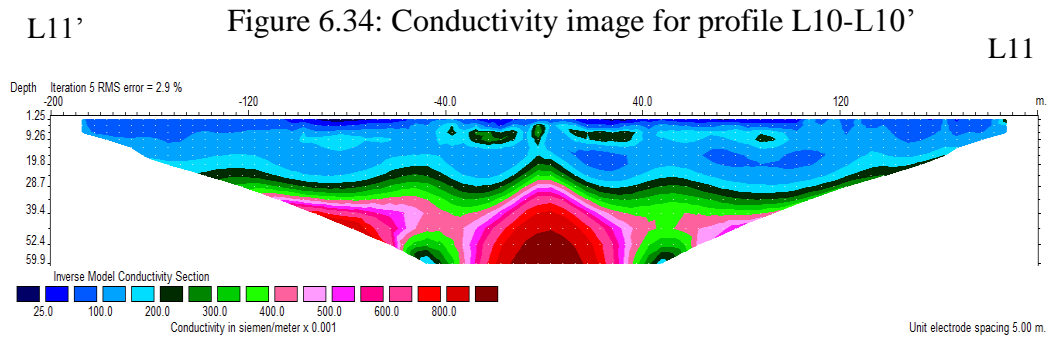


Figure 6.35: Conductivity image for profile L11-L11'

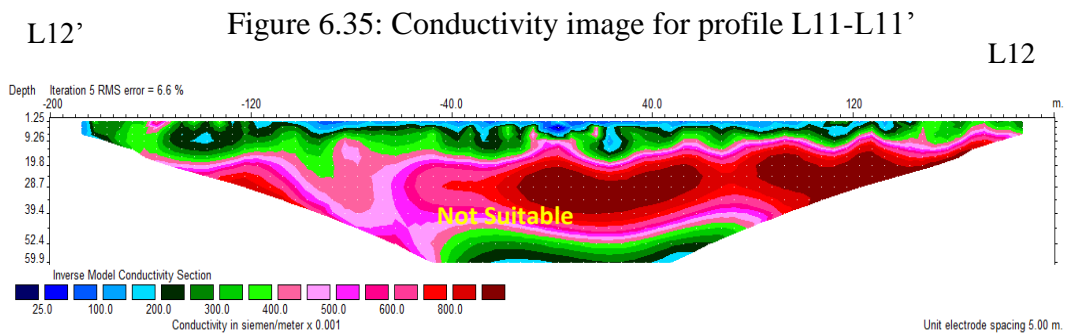


Figure 6.36: Conductivity image for profile L12-L12'

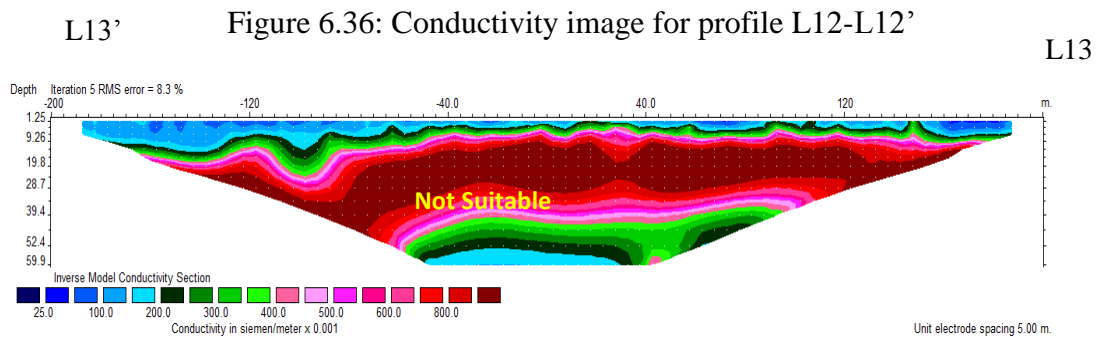


Figure 6.37: Conductivity image for profile L13-L13'

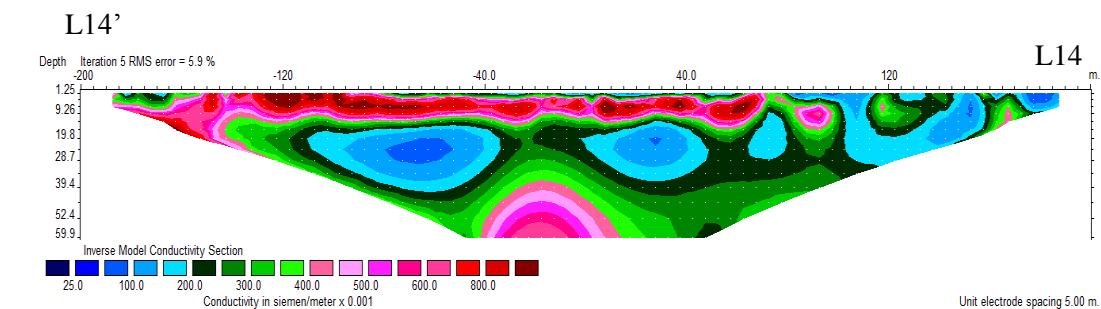


Figure 6.38: Conductivity image for profile L14-L14'

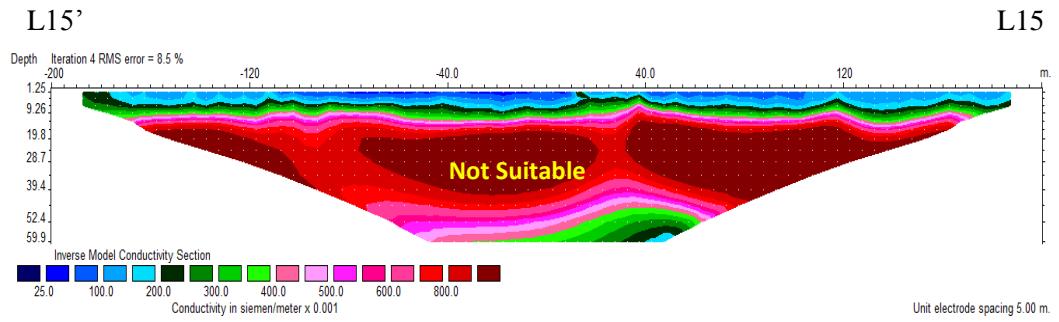


Figure 6.39: Conductivity image for profile L15-L15'

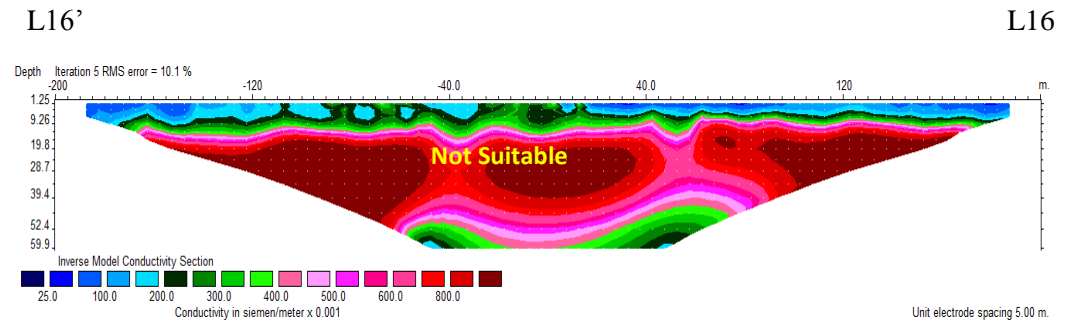


Figure 6.40: Conductivity image for profile L16-L16'

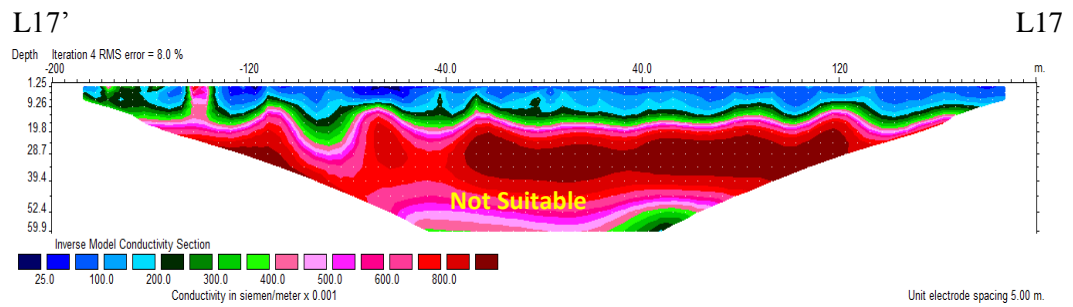


Figure 6.41: Conductivity image for profile L17-L17'

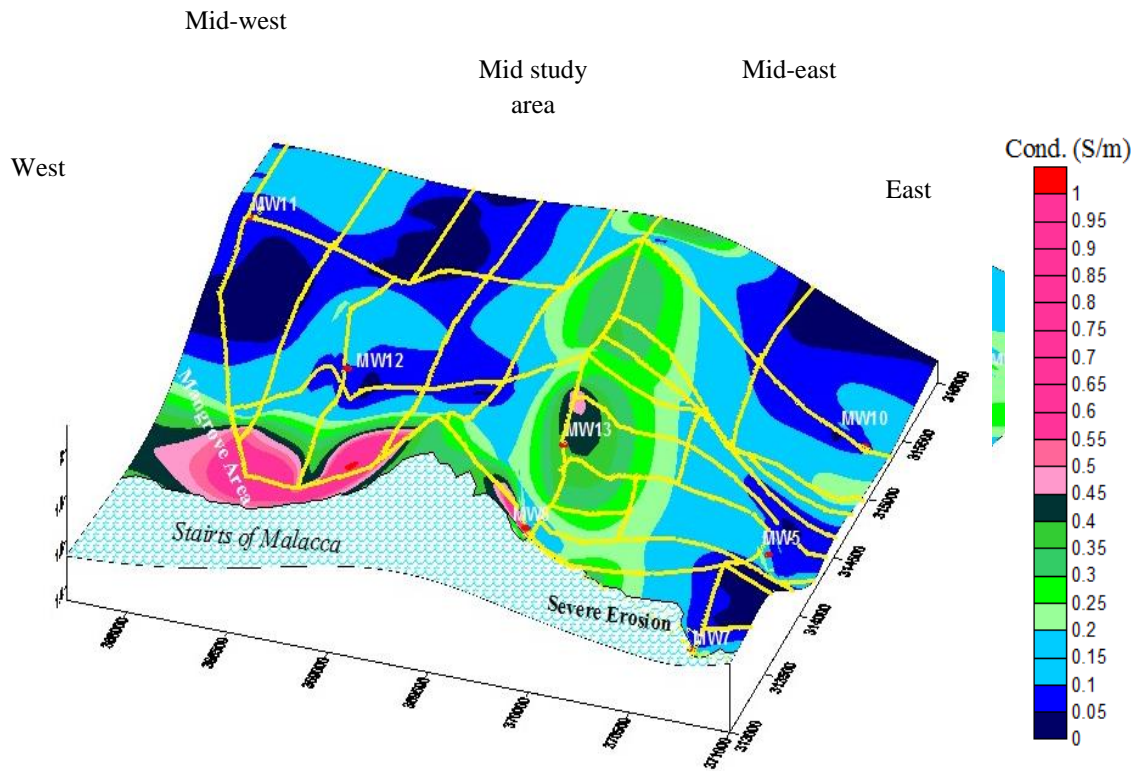


Figure 6.42: Conductivity distribution relative to elevation at 1.25 m depth and agriculture drainage system

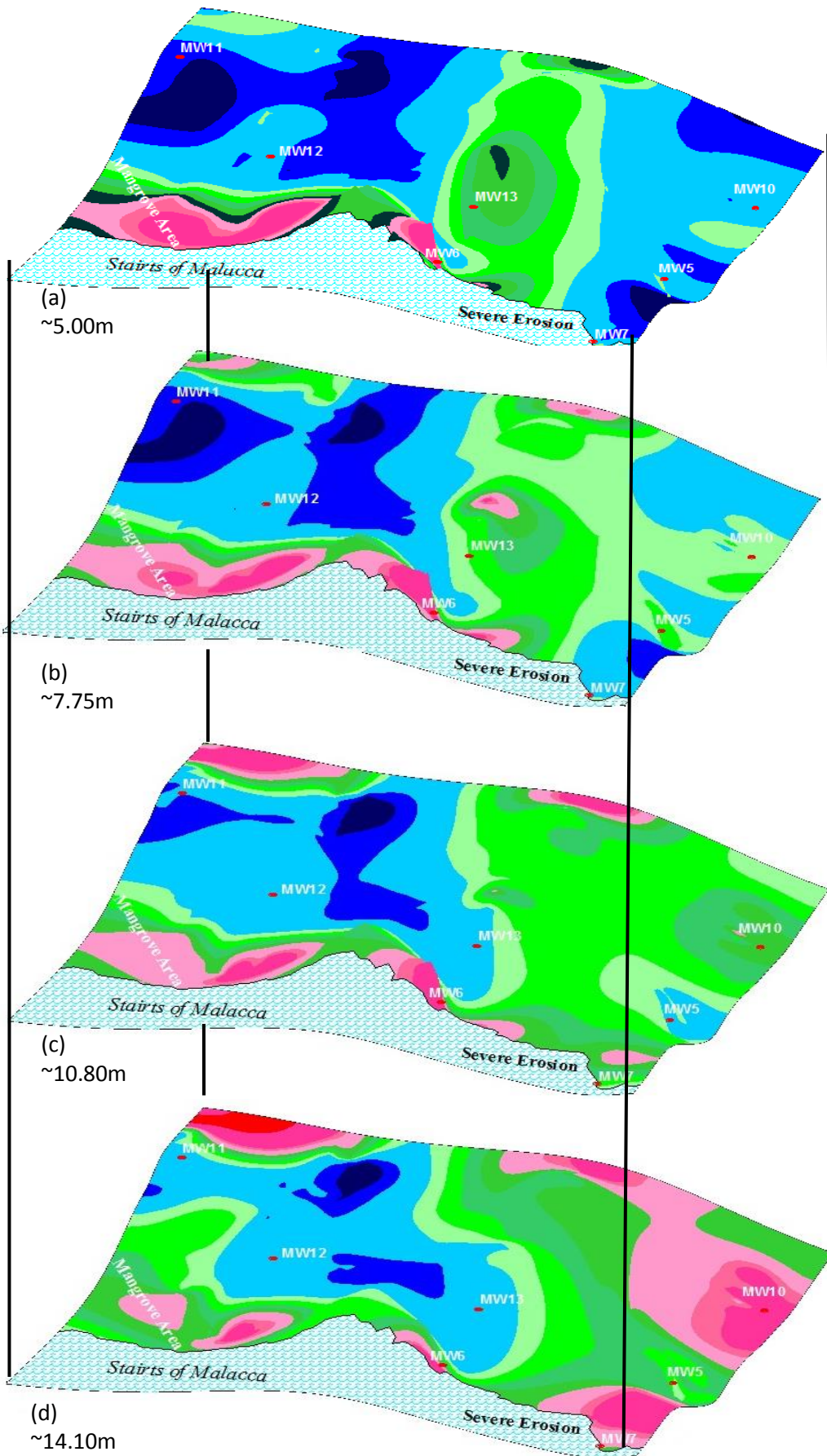


Figure 6.43: Conductivity distribution relative to elevation at 5.0 to 14.10 m depth

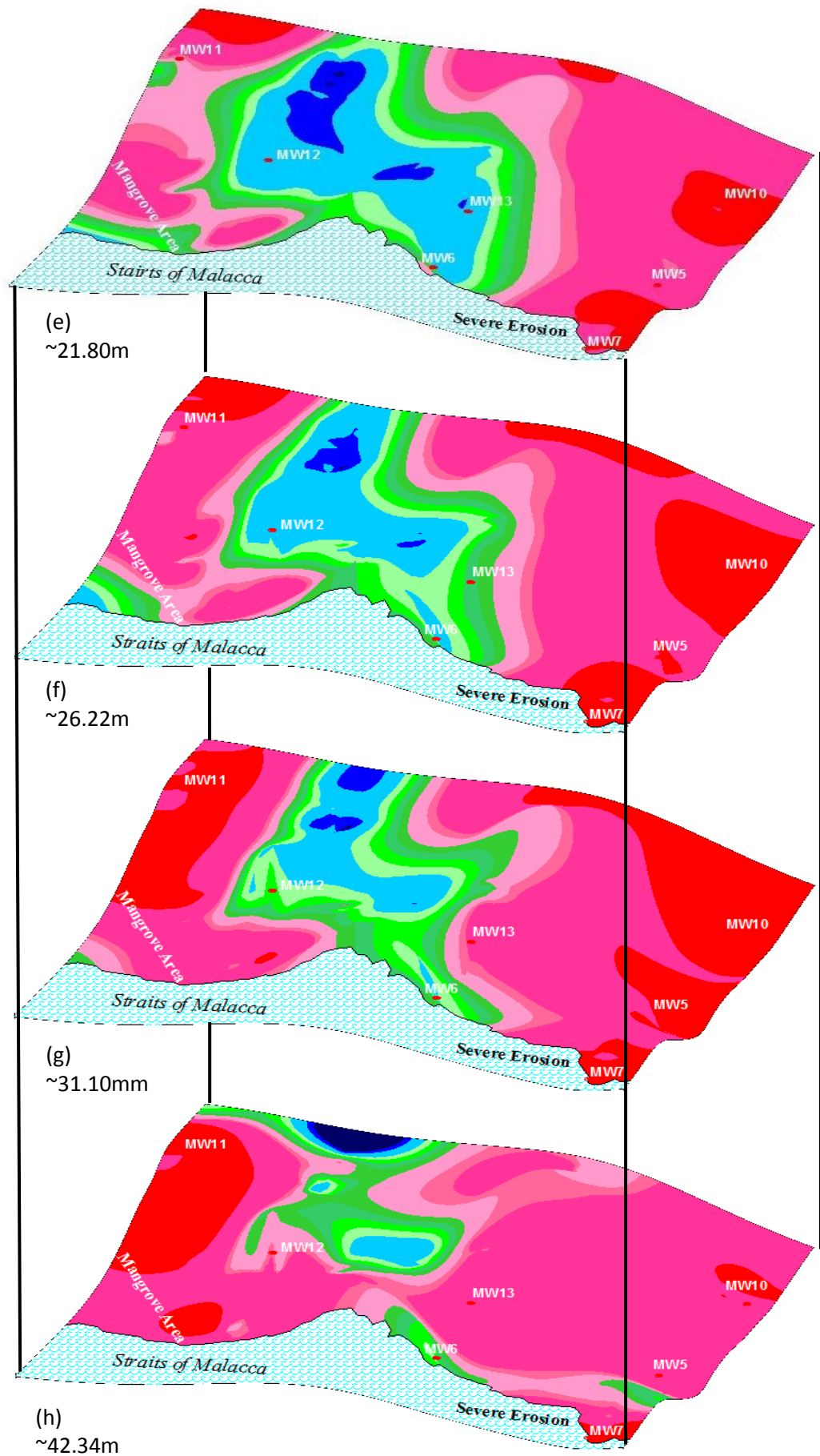


Figure 6.44: Conductivity distribution relative to elevation at 21.80 to 42.34 m depth

Table 6.3: Summary of conductivity distributions for the suitability of oil palm tree towards salinity and area coverage/dominancy

| Vertical Depth of Water Zone (m) | Horizontal Area Coverage (Km <sup>2</sup> ) of suitability of oil palm tree toward salinity |   | Suitability Area Dominancy | Remarks  |
|----------------------------------|---|---|----------------------------|--|
|                                  | Suitable, C > 0.4 S/m (Blue colour)   | Moderate Suitable-Not Suitable, C < 0.4 S/m (Green-Red colours) |                            |  |
| 1.25                             | 11.07   | 3.25  | West and East              | Moderate suitable caused by seepage from main canal and agriculture drainage (Figure 6.40)                               |
| 5.0                              | 9.82  | 4.50  | West and East              | Moderate suitable caused by seepage from main canal and agriculture drainage [Figure 6.41 (a)]                           |
| 10.80                            | 4.25  | 10.07   | West to Middle             | Moderate suitable to not suitable caused by seawater intrusion mostly from severely eroded area [Figure 6.41 (b)]        |
| 14.10                            | 3.75  | 10.57   | West to Middle             | Moderate suitable to not suitable caused by seawater intrusion mostly from severely eroded area (east) [Figure 6.41 (c)] |
| 21.80                            | 2.5   | 11.82   | Middle                     | Moderate suitable to not suitable caused by seawater intrusion [Figure 6.41 (d)]   |
| 31.10                            | 2.0   | 12.32   | Middle                     | Moderate suitable to not suitable caused by seawater intrusion [Figure 6.42 (f)]   |
| 42.34                            | 1.0   | 13.32   | -                          | not suitable caused by seawater intrusion [Figure 6.42 (h)]  |

Conductivity can be converted into TDS by using Equation (5.3). Table 6.4 shows the TDS value for the suitability classification for oil palm plantation in the area.

Table 6.4: TDS value for the suitability classification for oil palm plantation

| Conductivity (S/m)                                 | $C < 0.2$ S/m      | $0.2$ S/m $< C < 0.4$ S/m                 | $C > 0.4$ S/m       |
|--|--------------------|---|---------------------|
| <b>Sustainable status for oil palm cultivation</b> | Suitable           | Moderately Suitable                       | Not Suitable        |
| <b>TDS (mg/L) derived from equation (3)</b>        | TDS $< 5,300$ mg/L | $5,300$ mg/L $< \text{TDS} < 12,000$ mg/L | TDS $> 12,000$ mg/L |

### **6.5 Impact of sea-level rise to groundwater salinity and the suitability of oil palm cultivation towards salinity in Carey Island**

The effects of groundwater salinity due to seawater intrusion for the two types of land cover revealed that saline water can be found at a depth of 10 m at the east of unconfined aquifer (the coastal area experiencing severe erosion). Compared to the west area, the saline groundwater affected by seawater intrusion was found at 21 m from the ground surface. This situation has resulted in different limitations of groundwater suitability based on salinity tolerances for oil palm. The west area has thicker (31 m) suitable water for oil palm compared with the east (14 m). The prediction on the sea-level rise by IPCC (2007) in the twenty-first century around the world stated that the sea level rise will cause an increase in the seawater intrusion to the groundwater system at coastal areas. The local scenario sea-level rise prediction study showed that the mean sea-level rise rates at Port Klang (24 km away from Carey Island) using Special Report on Emissions Scenarios B1, A1B and A2 scenarios is 0.387 m. The prediction is based on the predicted slope from 2001 to 2100 (California Hydrologic Research Laboratory 2010). The unconfined aquifer facing the severe erosion area (profile resistivity lines near MW7, MW10 and MW5) showed that the groundwater level measured from the mean sea level is with the value of 0 to 0.3 m with TDS value of 12,000 mg/L (salinity

condition that can kill the oil palm) at the depth of 14 m from ground surface. Based on the Ghyben–Herzberg assumption, a 0.5 m increase in the sea level will cause a 20 m reduction in the thickness of the freshwater storage. The assumption predicted that this area will become unsuitable for oil palm plantation much earlier than the area on the north-west which still has mangrove forest. The root zone system of the oil palm can reach down until 1 to 6 m where this zone is in the water saturated condition with the high groundwater table between 0.738 m and 1.560 m from ground level data. This situation will caused unsuitable condition for oil palm cultivation. The current phenomenon in the unconfined groundwater aquifer system at the severely eroded area is summarized in Figure 6.45.

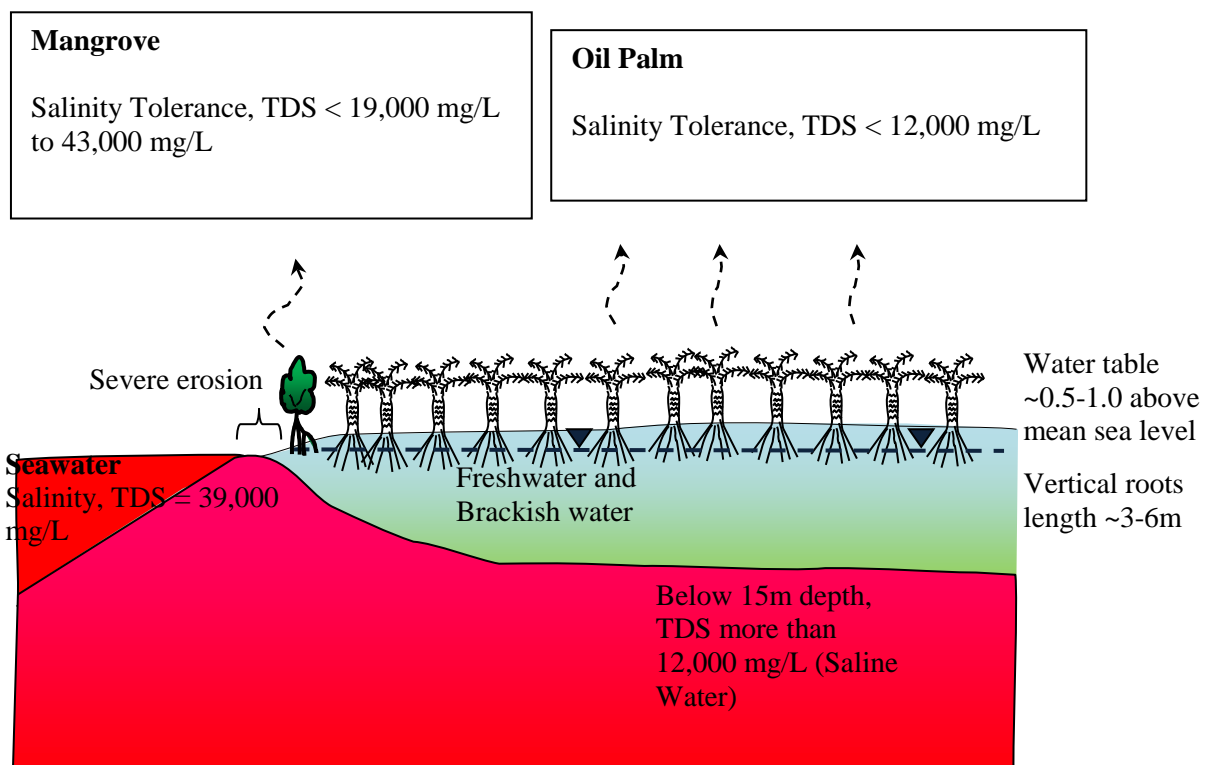


Figure 6.45: Diagram shows the interaction between severe erosion, mangrove and oil palm in Carey Island

## 6.6 Summary

The dominance of water brackishness/salinity is due to seepage from the agriculture drainage especially the main canal. The freshwater contamination in the shallow aquifer is caused by saline water infiltrating from the agriculture drainage.

The study also presented the current limitations and suitability of oil palm towards salinity. This is critical especially in the unconfined aquifer facing the severe coastal area. 3-D conductivity model showed conductivity values that are not suitable for oil palm plantation at a depth of 14 m in the east area. In the west area, the conductivity value remained suitable for the plantation at a depth of 31 m. The east area will be more vulnerable to seawater intrusion due to sea level rise in the future. Based on the Ghyben–Herzberg assumption, it is predicted that this area will become unsuitable for oil palm plantation much earlier than the mangrove-preserved area which still have mangrove forest in the west.

3-D conductivity model revealed the difference in salinity degree of the groundwater for oil palm in Carey Island. Factor controlling groundwater salinity distribution and oil palm tolerance towards groundwater salinity is caused by different type of surface characteristics between the west and the east area. The east area has a low surface elevation. No mangroves covered the coastal area, and it has more drainage than the west area. Surface characteristics in the east area naturally provide a more conducive environment for seawater intrusion to penetrate into the groundwater system than compared to the west area. A classification of TDS values for oil palm suitability is derived from the correlation of groundwater system in an unconfined area on Carey Island. Oil palm suitability classification uses TDS value where  $TDS < 5,300$  mg/L to be suitable,  $5,300$  mg/L  $< TDS < 12,000$  mg/L as moderately suitable, and  $TDS > 12,000$  mg/L as unsuitable. This classification can be used in the future to assess groundwater salinity for oil palm cultivation suitability by using the TDS value.